J Mater Cycles Waste Manag (2018) 20:914–924
https://doi.org/10.1007/s10163-017-0658-5

ORIGINAL ARTICLE

Characterization of poly(lactic acid) biocomposites filled with chestnut shell waste

M. Barczewski[1] · D. Matykiewicz[1] · A. Krygier[1] · J. Andrzejewski[1] · K. Skórczewska[2]

Received: 1 September 2016 / Accepted: 1 August 2017 / Published online: 11 August 2017
© The Author(s) 2017. This article is an open access publication

Abstract The aim of this study was to determine thermal and mechanical properties and applicability of ground chestnut shell waste as a filler for poly(lactic acid) composites. The used amount of filler was ranging from 2.5 to 30 wt%. Spectroscopic analysis of composites and its ingredients was conducted by means of FT-IR method. The mechanical and thermal properties of the composites were determined in the course of static tensile test, Dynstat impact strength test, DMTA analysis, and DSC method. The fractured surface morphology of biocomposites was evaluated by SEM analysis. Incorporation of the filler influenced the overall mechanical properties of the composites characterized by high stiffness and lowered impact resistance. Fabricated composites with different amounts of non-reactive natural waste filler exhibited acceptable mechanical and thermal properties. Therefore, these composites can be used as eco-friendly, biodegradable materials for low-demanding applications.

Keywords Poly(lactic acid) · Natural composites · Mechanical properties · Structure

Introduction

Increasing impact of the plastic products on the development of human life standard is connected with a long-term expansion of petroleum-based polymers. Despite trials of the reducing polymeric waste and strong restrictions concerning storage and product end-life cycle performance, the amount of the non-degradable polymer gradually has become ballast for the environment. Therefore, the endeavor of introducing biodegradable polymers in industrial-scale production gained ground among scientists [1]. The area of biodegradable material application is continuously extending thanks to their improving properties which in many cases resemble petrochemical polymers. In spite of many studies concerning the usage of biodegradable polymers, such as poly(lactic acid) (PLA) [2–10], poly(butylene adipate-*co*-terephthalate (PBAT) [11–13], polypropylene carbonate (PPC) [14–16], and starch [17–20], their commercial application is still not very common. Packaging industry appears as a branch which due to relatively low expectations towards mechanical properties allows for wide application of fully biodegradable polymers on a bigger scale [5]. The low thermo-mechanical stability of green composites, next to relatively high price, became their biggest disadvantage in comparison to petroleum-based non-biodegradable polymers [5, 13]. Therefore, it is well founded to use recycled thermoplastic biodegradable polymers as a matrix for composites filled with organic and inorganic fillers [7, 11].

Except for the application of the specially prepared fiber-like natural fillers (e.g., bamboo, kenaf, jute and flax), great attention is placed on incorporation of agricultural waste materials into polymeric matrix [2, 21–25]. Extensive studies showed that presence of the natural fillers in biodegradable polymers may strongly accelerate biodegradation process thanks to faster hydrolysis followed by oxidation of both biopolymer, as well as the filler. Moreover, presence of natural filler increases water absorption, which highly influences biodegradation process of the composites, in comparison to neat polymer. In case of natural composites

✉ M. Barczewski
mateusz.barczewski@put.poznan.pl

[1] Polymer Processing Division, Institute of Materials Technology, Poznan University of Technology, Piotrowo 3, 61-138 Poznan, Poland

[2] Faculty of Chemical Technology and Engineering, University of Science and Technology in Bydgoszcz, Seminaryjna 3, 85-326 Bydgoszcz, Poland

based on non-degradable polymers, hydrolysis under normal environment conditions will be reduced only to the particles of the natural filler; hence, polymer matrix becomes only physically fragmented and eroded [25]. The application of the chestnut shell waste as a natural filler for polymer composites had been previously reported. Kaymakci et al. investigated the effect of chestnut shell on mechanical properties, as well as dimensional stability of the polypropylene based on composites with application of maleic anhydride–polypropylene (MAPP) as a coupling agent. The results presented in their study showed that the incorporation of MAPP into natural composites based on hydrophobic polymeric matrix strongly reduces water absorption and increases mechanical properties of the modified composites [26]. Another study which presents the application of chestnut shell waste as a filler was presented by Wu et al., who focused on the development on poly(butylene succinate)-based biocomposites [27]. It should be noticed that no literature studies concerning the modification of the poly(lactic acid) by chestnut shell powder were presented in the literature. Therefore, the aim of this study is to determine thermal and mechanical properties of poly(lactic acid) filled with chestnut shell powder waste composites and potential applications resulting from them.

Experimental

Materials and sample preparation

The commercial injection molding grade poly(lactic acid) (PLA) Ingeo™ 3001D with a melt flow rate (MFR) of 22 g/10 min (210 °C, 2.16 kg) supplied by Nature Works (USA) was used in our experiments.

Preliminary preparation of the chestnut shell waste filler (CN, *Aesculus hippocastanum* L.) included rinsing in running distilled water and drying at 50 °C for 24 h. First disintegration was processed in a low-speed mill cutter Shini SC-1411 and then milled in high-speed mill Retsch GM 200 ($n = 2000$ rpm). Application of the two-step milling allows the preparation of non-degraded natural filler for PLA-based biocomposites. The obtained waste chestnut shell powder was sieved by vibratory sieve shaker ANALYSETTE 3 Pro equipped with 200-μm-mesh size sieve. Characterization of particle size distribution was evaluated using laser particle sizer Fritsch ANALYSETTE 22 apparatus operated in the range of 0.08–2000 μm.

PLA pellets and CN powder were premixed using a high-speed rotary mixer Retsch GM200 ($t = 3$ min, $n = 1000$ rpm) with different amounts of filler (2.5, 5, 10, 20, and 30 wt%). Next, all blends were mixed in a molten state using a ZAMAK 16/40 EDH twin screw co-rotating extruder that operated at 190 °C and 100 rpm, and pelletized after cooling in a water bath. The normalized specimens for tensile and impact strength test were prepared with a Engel HS 80/20 HLS injection molding machine operated at 190 °C. Injection molding process was realized with the following parameters: mold temperature $T_{mould} = 25$ °C, injection speed $V = 70$ mm/s, forming pressure $P_f = 5$ MPa and cooling time $t = 45$ s. Materials were every time dried in a vacuum at 50 °C for 24 h before being mixed in molten state. The samples were described as PLA, 2.5CN, 5CN, 10CN, 20CN, and 30CN, adequately to incorporated amount of chestnut shell waste powder.

Methods

The thermal stability of chestnut shell was determined by thermogravimetric analyses (TGA) with temperature set between 30 and 800 °C at a heating rate of 10 °C/min under nitrogen and air atmospheres using a TG 209 F1 Netzsch apparatus with ceramic pans. The initial decomposition temperature T_5 was determined as a temperature at which the weight loss was 5%, also temperature T_{50} at which weight loss is equal to 50% was designated. The residual mass (ΔW%) was defined at about 800 °C.

The FT-IR measurements were conducted by means of a Fourier transform spectrometer Bruker Vertex 70, at an ambient temperature (23 °C). To analyze the ground chestnut shell, poly(lactic acid) and 30CN composite surfaces, Attenuated Total Reflectance Fourier Transform Infrared Spectroscopy (ATR FT-IR) was used. In all cases, a total of 64 scans at a resolution of 1 cm^{-1} was used to record the spectra. All spectra, including the CO_2 one, were submitted to weather correction.

Differential scanning calorimetry (DSC) measurements were performed using a Netzsch DSC 204 F1 Phoenix® apparatus with aluminum crucibles and approximately 5-mg samples, under nitrogen flow. All the samples were heated up to 190 °C and held in a molten state for 5 min, followed by cooling down to 20 °C. Heating and cooling rates were equal to 10 °C/min. This procedure was conducted twice to evaluate the DSC curves from the second melting procedure and gain broad information about PLA and PLA–CN composites' thermal properties.

Mechanic properties of pure PLA and PLA composites were evaluated in static tensile test according to European standard ISO-527 by means of Zwick Roell Z020 TH ALL-round Line universal testing machine with 20 kN nominal force. Tests were carried out with 50 mm/min cross speed. Each evaluation was prepared for 15 test specimens.

The impact strengths of the unnotched samples with 10 × 4 × 15 mm dimensions were measured by the Dynstat method according to DIN 53435 standard. Presented

impact strength values are arithmetic mean calculated from 15 measurements.

The dynamic mechanical properties of the composites, with $10 \times 4 \times 50$ mm dimensions, were studied using DMTA methods in a torsion mode, operating at frequency $f = 1$ Hz in the temperature range between 25 and 100 °C, and at heating rate 2 °C/min. These methods applied very small sinusoidally varying strains to test the material at constant frequency and constant heating rate. The stress is defined as storage modulus G', loss modulus G'', and loss factor tanδ [28]. The position of tanδ at its maximum was taken as the glass transition temperature (T_g).

The structure changes evaluation caused by the incorporation of the filler was determined by scanning electron microscopy (SEM). The samples' fracture surfaces were examined and digitally captured using a scanning electron microscope Zeiss Evo 40. The electron accelerating voltage of 12 kV was applied. Prior to the tests, all the specimens were sputtered with a layer of gold. The magnifications of 1000× and 8000× were used.

Results and discussion

Characterization of the chestnut shell filler

In Fig. 1, particle size distribution function (*Q3(x)*) and its derivative (*dQ3(x)*) as a function of particle size (*x*) were presented. The arithmetic mean size of hybrid filler fraction after milling was equal to 10.71 µm. Additionally, characterization of organic filler particle size and shape was performed by means of scanning electron microscopy (SEM) (Fig. 2).

In Figs. 3 and 4, plots of weight loss vs. temperature and their derivatives (DTG) are presented. Temperatures recorded at two characteristic mass loss values (5 and 50%) were assigned as T_5 and T_{50}. The values of T_5 and T_{50} for chestnut filler determined in nitrogen atmosphere were 202 and 357 °C, and in air atmosphere they were 169 and 302 °C, respectively. Peak temperature of DTG curves and maximum rate of degradation filler were 307 °C and 5.1%/min in inert atmosphere and 283 °C and 5.7%/min in oxygen atmosphere.

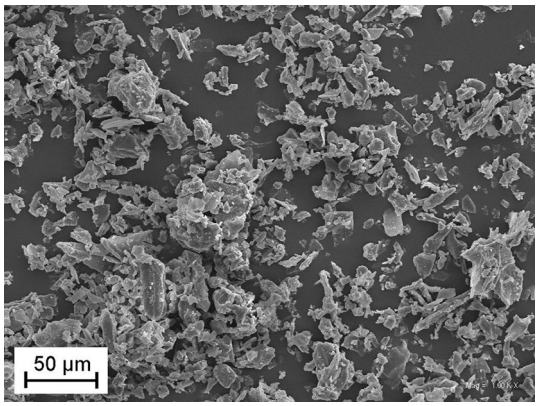

Fig. 2 SEM image of milled chestnut shell powder, magnification 1000×

The ΔW% was defined as 36.7% in nitrogen and 5.8% in air atmosphere. The thermal stability of chestnut filler was sufficient to proceed with melt processing.

Spectroscopic analysis of composites and its ingredients

The FT-IR spectra of ground chestnut shell, PLA, and composite containing 30 wt% of CN are presented in Fig. 5. In CN spectra the broad absorption band at 3000–3500 cm^{-1} indicates bonded hydroxyl (–OH) groups existing in the natural filler [29]. Peak observed at 2900 cm^{-1} corresponds to C–H stretching band originating from aliphatic moieties in cellulose and hemicellulose [30]. The peak at 1720 cm^{-1} in CN spectra is related to C=O stretching band from ester linkage of carboxylic group in the lignin ferulic and p-coumaric acids [31]. The observed peak at 1606 cm^{-1} corresponds to C=C aromatic stretching band and confirms the presence of lignin in the natural filler. Double absorption peak at wavenumbers of 1093 and 1068 cm^{-1} is assigned to C–O stretching band from ether and alcoholic group [31, 32]. In case of PLA, absorption peaks at wavenumbers: 3510, 2995, 2950, 1749, 1450, 1362, and 1053 cm^{-1} are related to C–O–O–H stretching, C–H aliphatic stretching, C–H aliphatic stretching (doublet), C=O bending, $–CH_2$ bending, C–H bending, and C–O stretching, respectively [33, 34]. The absorption

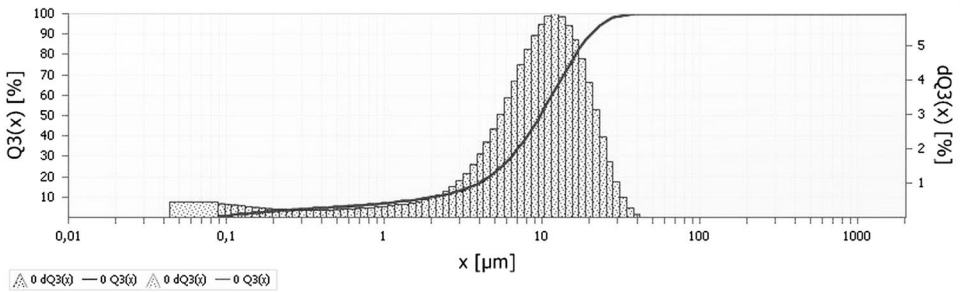

Fig. 1 Particle size distribution of milled and sieved chestnut shell

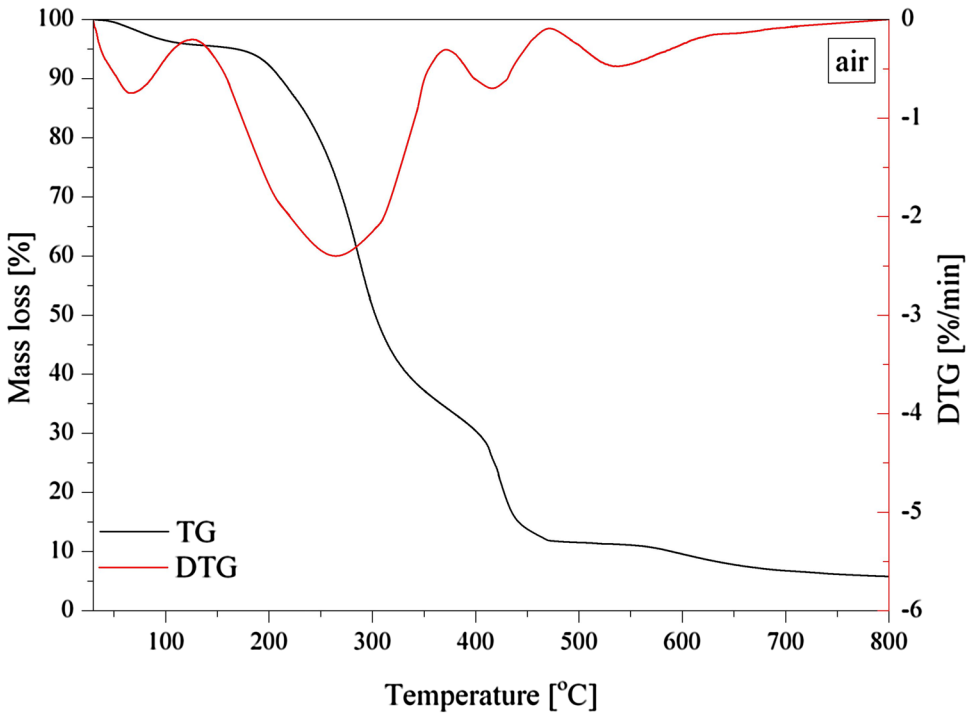

Fig. 3 TG and DTG curves of chestnut filler investigated under nitrogen atmosphere

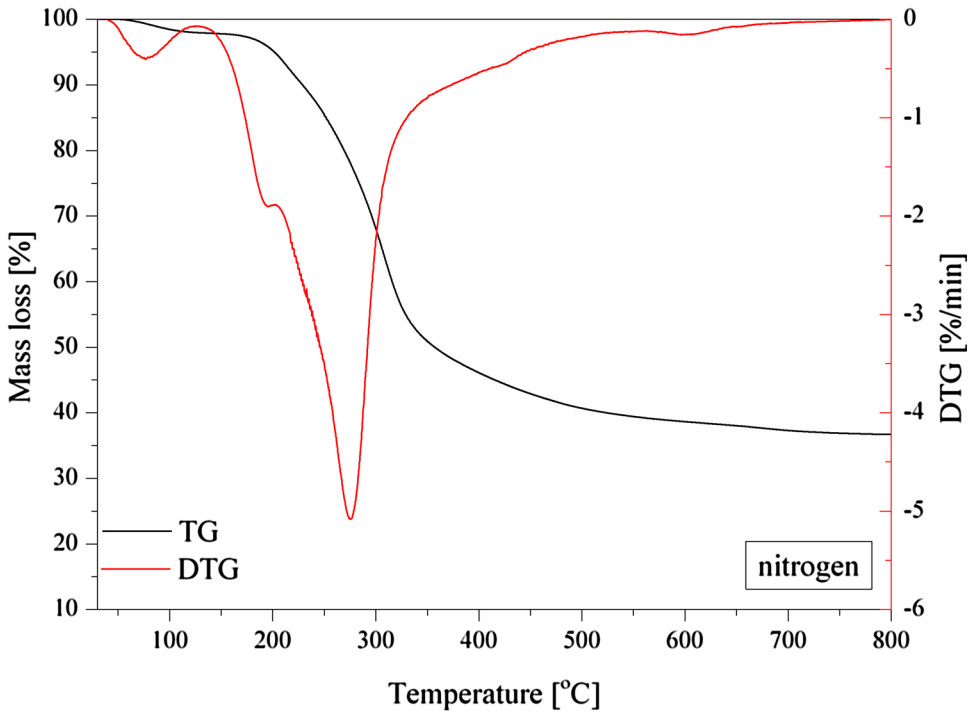

Fig. 4 TG and DTG curves of chestnut filler investigated under air atmosphere

bands at 1207 and 920 cm^{-1} are associated with allyl-ketone chain vibration and flexural C–H bond vibration and are representatives of the PLA crystalline structure [35, 36]. In contrast to pure PLA, the 30CN composite sample exhibits distinct peaks at mentioned wavelengths which correspond to crystalline structure. This is due to a nucleating ability of ground chestnut shells incorporated into PLA. These results are in a good agreement with crystallinity degree values evaluated within DSC experiments, which will be discussed later. The poly(lactic acid)-based composites containing various amount of ground chestnut waste were prepared without coupling agents and preliminary chemical treatment of the natural filler. Therefore, no chemical interactions and additional peaks at FT-IR spectra of composite containing

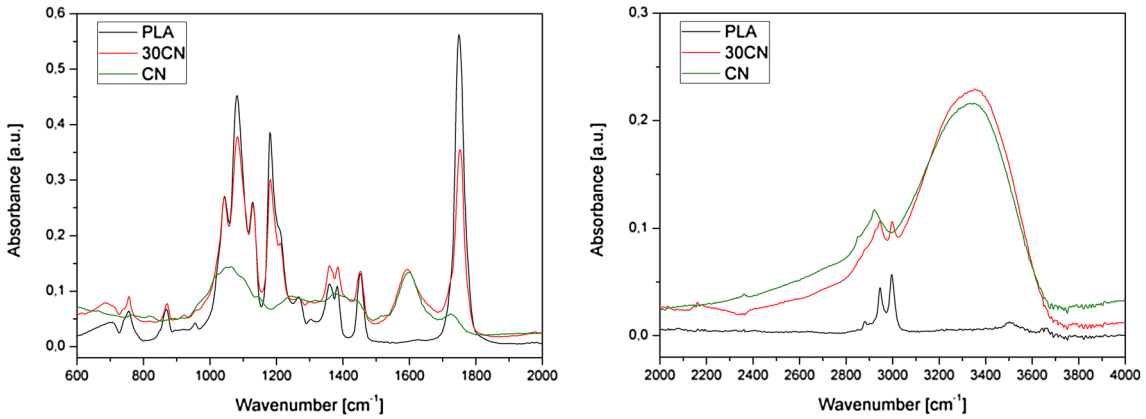

Fig. 5 Absorbance vs. wavenumber ATR FT-IR spectra of ground chestnut shell, PLA, and 30CN composite in a range from 600 to 4000 cm^{-1}

30 wt% of CN were observed. The 30CN FT-IR spectrum presents peaks originating from both PLA and chestnut natural filler. Lowered absorbance at the wavelengths corresponding to poly(lactic acid) in case of the 30CN sample is attributed to lower amount of polymer in composite. What is important, despite the presence of 30 wt% amount of the natural filler with high ability for moisture and water adsorption, no significant effects of hydrolytic degradation of PLA in the composite during processing was observed. There was no shift of the peak at 1081 cm^{-1}, which may suggest the presence of hydrolysis due to hydrogen bonding or nucleophilic attack by water molecules at –C–O– ester bonds. Shift of the 1749 cm^{-1} peak, corresponding to carbonyl group C=O band ascribed to ester bonds, was also negligible [37]. Therefore, it can be stated that it is not necessary to apply special methods of material drying or additional preprocessing of the composite pellets before melt processing, in comparison to pure PLA.

Thermal properties

DSC curves of PLA and PLA–CN composites obtained during second heating process are presented in Fig. 6. Three transformations comprised by DSC data were observed and analyzed: enthalpy relaxation corresponding to glass transition (about 58 °C), cold crystallization (near 106 °C), and melting of polymer matrix (168 °C). Additionally, DSC parameters, such as glass transition temperature (T_{g1}), cold crystallization temperature (T_c), melting temperature (T_m), melting enthalpy (ΔH_m), and

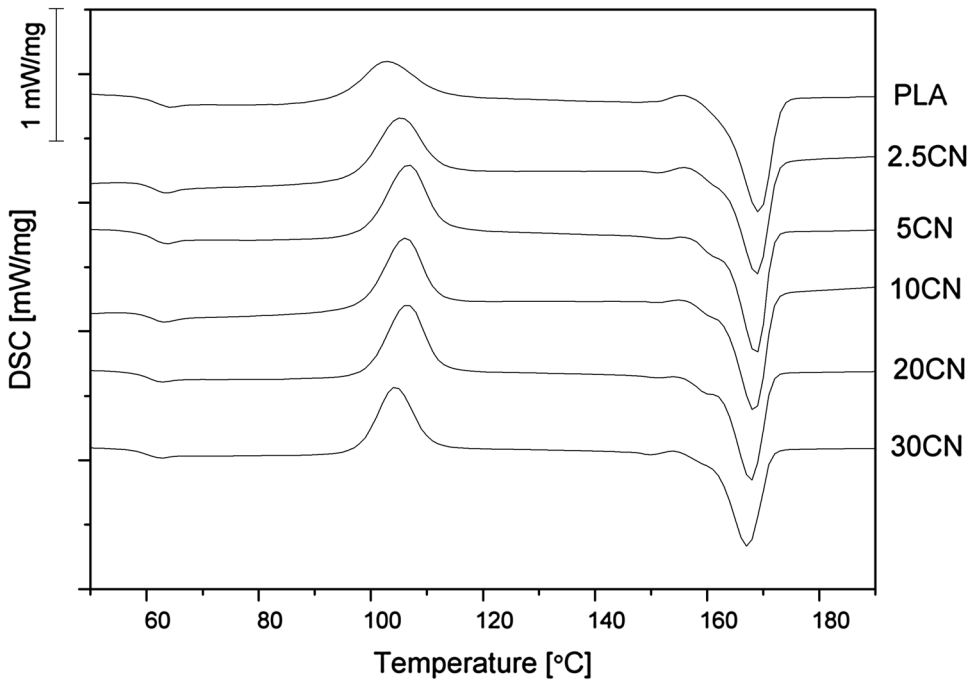

Fig. 6 DSC curves obtained from second heating of PLA and PLA–CN composites

crystallinity level (X_c), are listed in Table 1. The crystallinity degree of pure PLA and PLA–CN composites was calculated using the following equation:

$$X_c = [(\Delta H_m/(1-\Phi)\,\Delta H_o)]\,100\% \quad (1)$$

where ΔH_o is the melting heat of entirely crystallized PLA and its value is equal to 106 J/g [38], and Φ is the amount of filler. On the bases of the data presented, it is clearly visible that the incorporation of chestnut shell waste powder does not significantly influence glass transition temperature determined by DSC. Only in case of composite samples containing the highest amount of the filler small decrease of T_{gl} value was observed. Pure poly(lactic acid) reveals low crystallization ability; therefore, macromolecular chains are unable to arrange completely during rapid cooling. In effect, during PLA heating process, quenched polymer chains rearrange forming regions with higher crystallinity. What is more, cold crystallization temperature peak increases in comparison to pure PLA, and achieves maximum value of 106.7 °C for 5 wt% of CN. At the same time recorded T_c values for the highest filler concentration, i.e., 30 wt%, lowered and revealed value 104.4 °C. The lowered T_c for 30CN sample may have resulted from melt crystallization enhancement of PLA. High amounts of organic fillers with developed surface act as nucleating agents which promote regular arrangement of polymer chains and increase crystal growth during PLA-based composite cooling [10]. The heat of fusion values obtained during melting of PLA and PLA–CN composites remained at similar level. On the other hand, crystallinity level of PLA–CN composites calculated in accordance with Eq. 1 was significantly increased in comparison to pure PLA. For pure PLA, crystallinity level of 41.6% was measured; hence, for the highest CN content (30 wt% CN) X_c was equal to 49.2%. This phenomenon confirms nucleation ability of the incorporated organic filler particle. This is in good agreement with the work of Ouchiar et al. who proved that the use of adequate fillers may be a route to tuning the nanostructure of a polylactide [39]. Moreover, it can be stated that DSC results confirm FT-IR analysis, which reveals the presence of higher amount of crystalline phase in composite containing 30 wt% of the filler in comparison to pure PLA.

Table 1 Thermal parameters obtained from DSC during second melting

Name	T_{gl} (°C)	T_c (°C)	T_m (°C)	ΔH_m (J/g)	X_c (%)
PLA	59.1	103	169.1	44.1	41.6
2.5CN	59.4	105.3	168.8	42.8	41.4
5CN	58.9	106.7	168.7	46.6	46.2
10CN	59.1	106.2	168.3	44.9	47.0
20CN	58.1	106.4	167.8	40.5	47.7
30CN	57.6	104.4	167.1	36.5	49.2

Mechanical behavior of PLA and PLA composites

The results of mechanical properties obtained in the course of static tensile test and impact strength measurements are presented in Fig. 7. It may be seen that the incorporation of organic waste filler highly influenced the overall mechanical properties of PLA-based composites. The increasing content of ground chestnut shell led to gradual increase of the stiffness with simultaneous reduction of the composites' tensile strength. Pure PLA samples showed elasticity modulus value of approx. 3.1 GPa. For lower amounts of CN (up to 5 wt%), the samples' elasticity modulus values were similar to those recorded for pure PLA, and demonstrated average values of 3.1 GPa and 3.2 GPa, corresponding to 2.5CN and 5CN samples. Composites with higher filler concentrations, i.e., 10 wt% and more, showed stronger tendency to stiffness improvement, achieving the maximum of 30 wt% CN concentration, with E value of 3.8 GPa. According to the literature exploring this field, the Young's modulus may increase with an increasing level of crystallinity of the composite samples [40]. Opposite tendency may be observed when analyzing the influence of filler loading on the tensile strength of PLA composites. This phenomenon is characteristic of composite materials modified by particle-shaped fillers with size above 1 μm [41]. As this research proceeded, the tensile strength decreased from 69 MPa (pure PLA) to 40.8 MPa for composite filled with 30 wt% of CN. This effect may be attributed to weak bonding between the hydrophilic natural filler and hydrophobic polymer matrix. Moreover, the application of unmodified particle-shaped filler with broad particle size distribution may act as supplement crack indentation point [41]. The only exception was observed for composite samples containing 2.5 wt% of CN, where tensile strength was not influenced by the presence of the CN filler. Considering elongation values recorded at samples break, behavior which is typical for filled polymeric materials was noticed. Average elongation at break value determined for pure PLA, equal to 4.8%, decreased to 1.5% for highest CN content. What is more, increasing content of the CN filler caused reduction of the elongation at break inversely proportional to increased brittleness of the PLA–CN composite samples determined by Dynstat impact test [42]. More than 50% reduction of impact strength of PLA–CN composites was observed in comparison to pure PLA samples. To conclude, incorporation of natural powder filler with broad particle size distribution, without preliminary chemical treatment,

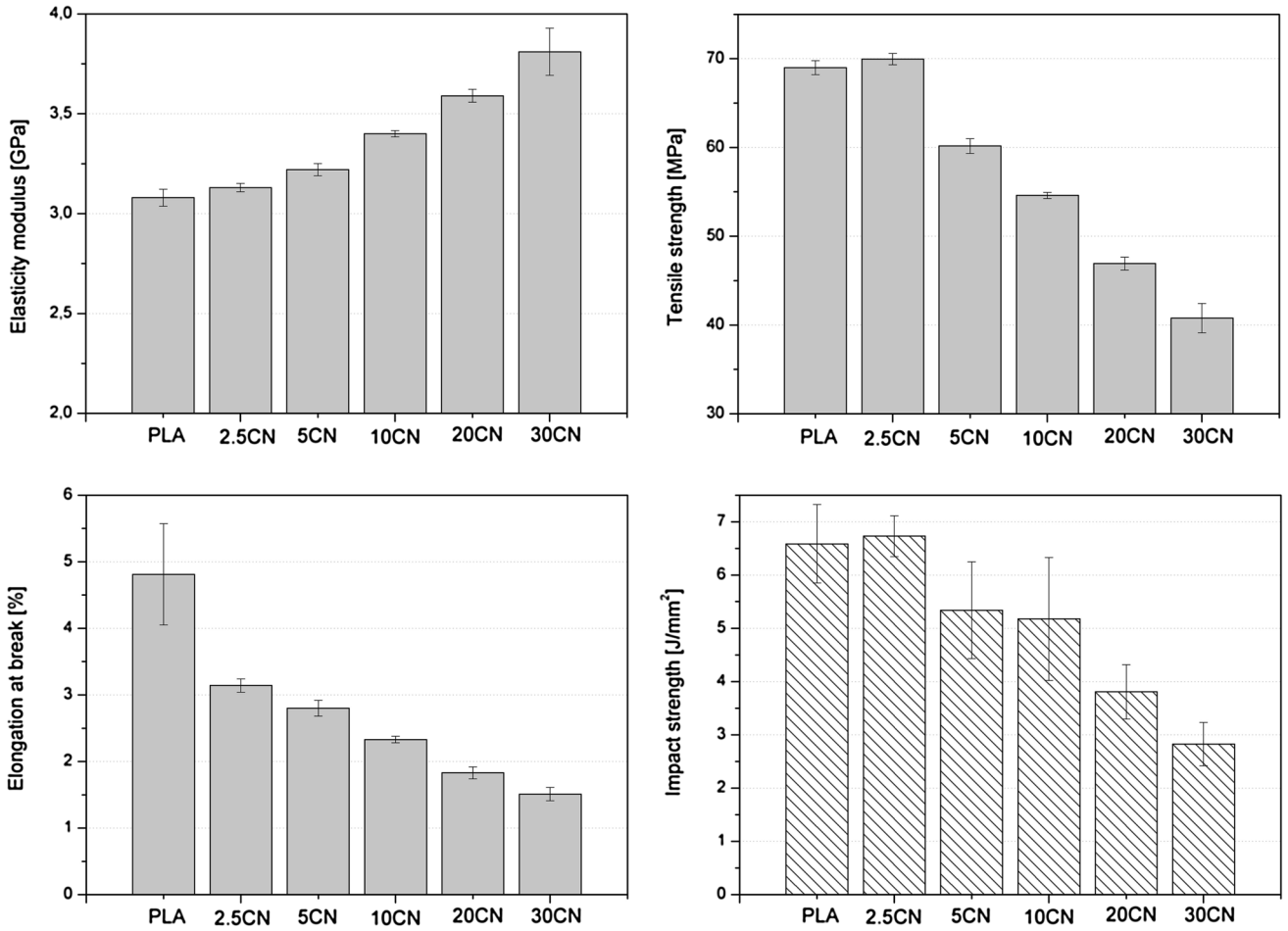

Fig. 7 Mechanical properties of pure PLA and PLA–CN composites

causes strong increase of the composite material stiffness and brittleness.

Dynamic mechanical properties

The dynamic mechanical thermal analysis was used to determine the influence of the filler content on the viscoelastic behavior of the composites, described by dynamic and damping properties. The storage modulus (G') represents the elastic portion of viscoelastic behavior connected with solid-state behavior of sample, whereas loss factor (tanδ) is a very useful parameter for detecting molecular transitions of the polymers and allows to relate DMTA results to interactions between components of polymer composites and blends [43, 44]. Plots of the storage modulus and loss factor versus temperature T for all samples are shown in Figs. 8 and 9. The values of storage modulus at room temperature as well as detailed information about glass transition temperature of the composites are given in Table 2. The highest value of G' (2340 MPa) was reported for the sample with the highest amount of ground chestnut shell in comparison with the reference sample PLA (1430 MPa). This phenomenon is in agreement with observed significant increase of Young's modulus determined by tensile test and suggests that particle-shaped filler have strong influence on the elastic properties of composite. Hence, the tanδ peak intensity for the composites decreases with an increase of CN content and this may confirm that the introduction of this filler hinders mobility of the PLA chains [40, 45]. Incorporation of particle-shaped filler into polymer matrix causes increase of the elasticity and decreases ability for mechanical energy dissipation; therefore, less energy will be used to overcome the frictional forces between molecular chains as to decrease mechanical loss [46]. This fact may be also attributed to increased crystallinity level of the composites in comparison to pure PLA. The addition of chestnut shell led to the slight lowering of the composite glass transition temperature (T_g), from 70 °C for pure PLA samples down to 68 °C for composites containing 30 wt% of ground chestnut shell. Decrease of the T_g may be attributed to insufficient interfacial adhesion between polymer and filler [47]. These results are also in good agreement with DSC investigations

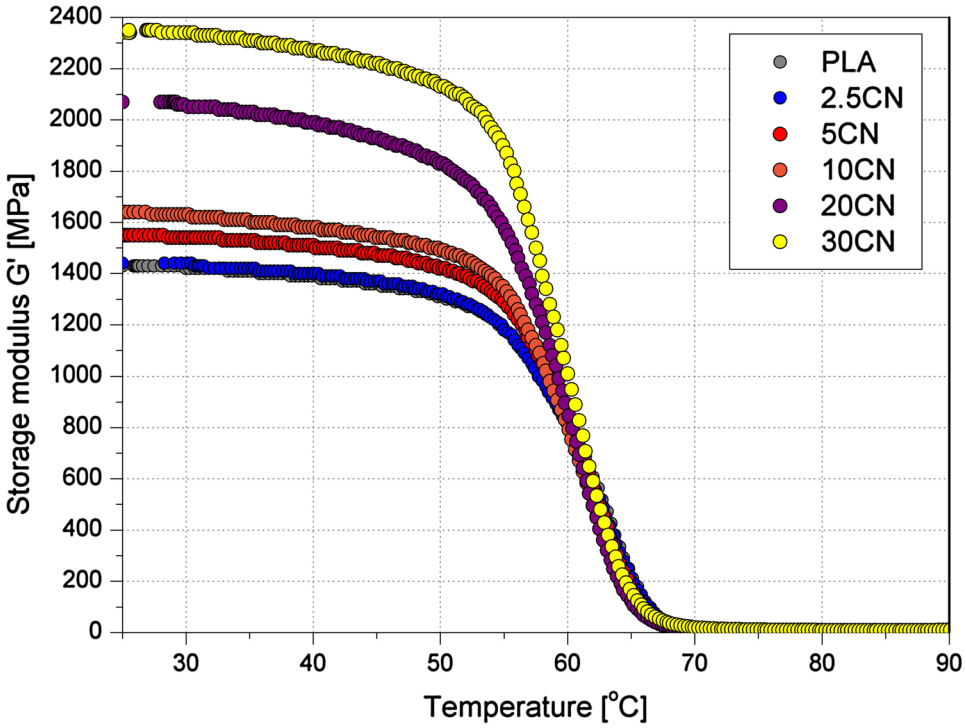

Fig. 8 Storage modulus vs. temperature of PLA and PLA–CN composites

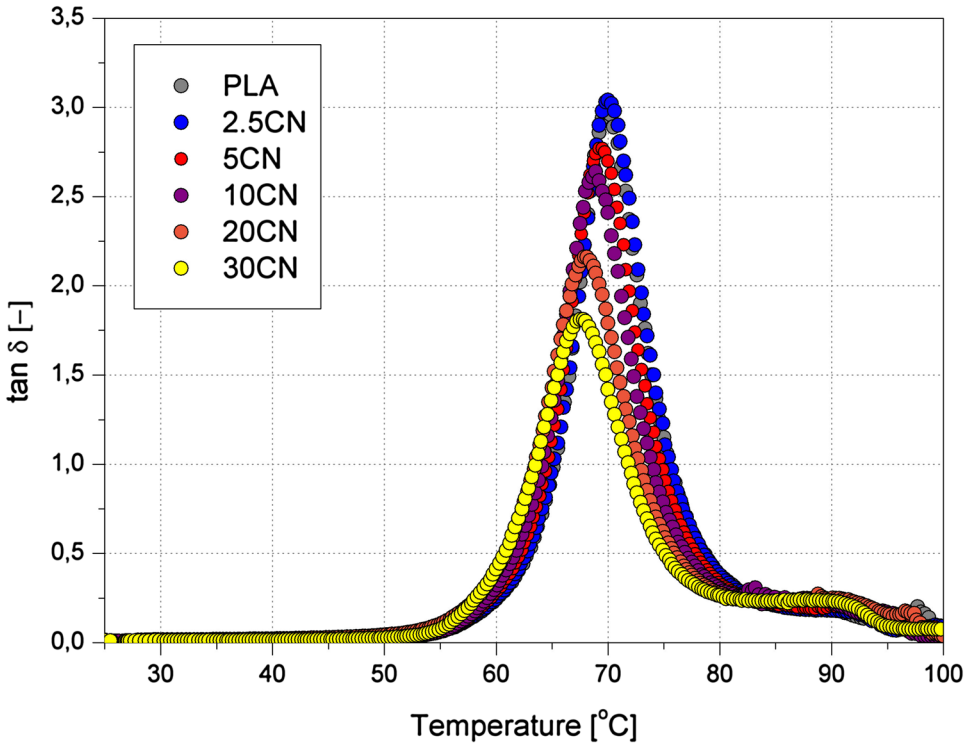

Fig. 9 Tanδ vs. temperature of PLA and PLA–CN composites

where similar tendency was observed. The glass transition temperature determines the range of polymer material usage. It is noteworthy that the fact that there are no significant changes in T_g values is favorable for application of composite product in standard room temperature usage.

Morphology analysis

The SEM micrographs of PLA and PLA–CN composites containing from 2.5 up to 30 wt% of the natural filler, made with magnification 1000×, are presented in Fig. 10.

Table 2 The values of PLA and PLA–CN composites storage modulus and glass transition temperature

Name	$G'_{25\ °C}$ (MPa)	T_g (°C)	tanδ at T_g (a.u.)
PLA	1430	70	2.97
2.5CN	1440	70	3.04
5CN	1550	68	2.77
10CN	1640	69	2.64
20CN	2070	68	2.16
30CN	2340	68	1.81

The observed dispersion of the organic filler in polymeric matrix was sufficient. Particles with various sizes were uniformly dispersed in polymeric matrix, which may be also confirmed by the low values of standard deviations of mechanical parameters determined by uniaxial tensile test. However, for 30CN composite, pullout cavities around bigger sized chestnut particles were observed. To determine the adhesion between polymer matrix and the filler, additional SEM microphotograph is presented in Fig. 11. It can be noticed that the saturation of the 20-μm chestnut particle by poly(lactic acid) was not significant. Most of the particles

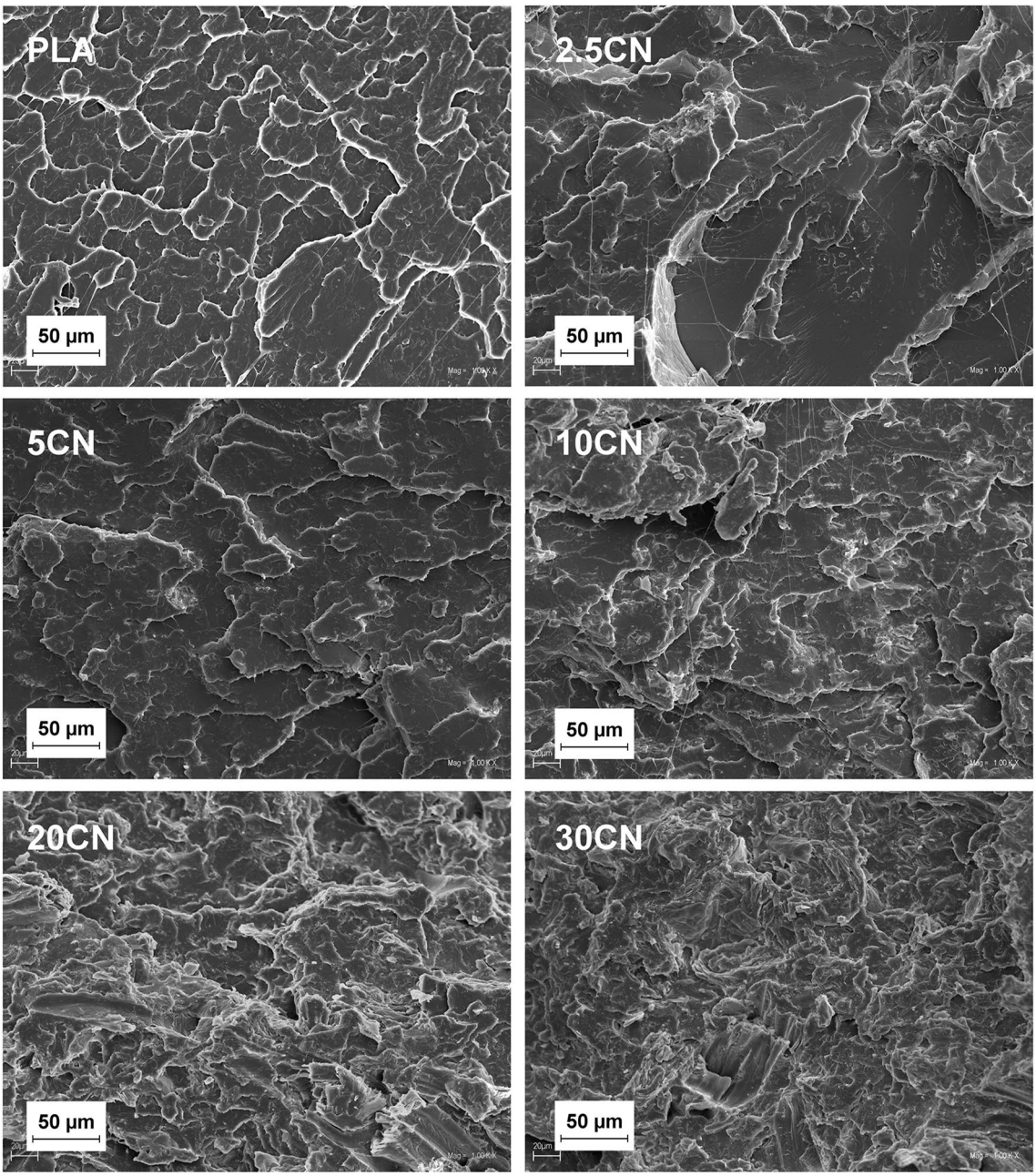

Fig. 10 SEM images of PLA and PLA–CN composites, magnification 1000×

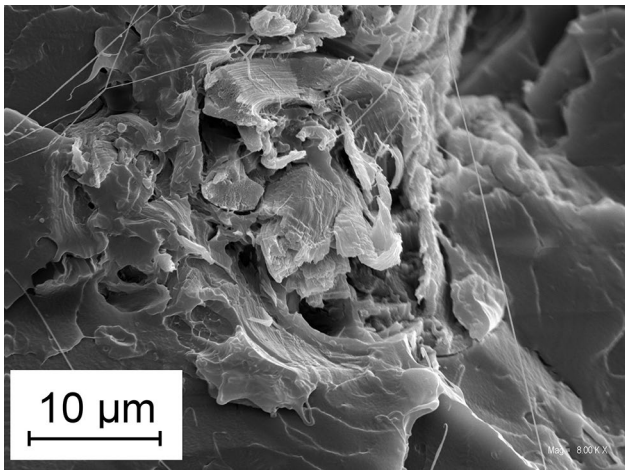

Fig. 11 SEM image of chestnut particle in PLA matrix, magnification 8000×

observed in Fig. 10 were not fully pulled out from the bulk but broken on the fracture surfaces; however, in Fig. 11, cavities between filler and polymeric matrix can be clearly seen. Despite both these phenomena occurring simultaneously, dominant effect on the mechanical properties of PLA-based composites may be caused by insufficient adhesion between polymer and filler. Analysis results of SEM images are in agreement with described significant increase of the brittleness of the composites (increased stiffness with general deterioration of remaining mechanical properties of the composites) in comparison to pure PLA, as well as lowered glass transition temperature determined by DSC and DMTA.

Conclusions

The aim of modern scientists is to explore new material solutions which would allow to reduce the negative impact of petrochemical polymers on the environment. Therefore, in this work the chestnut shell was used as non-reactive filler in poly(lactic acid) composites with the highest concentration at 30 wt%. Application of various measuring techniques, including: FT-IR, DSC, DMTA, SEM, and complex evaluation of mechanical properties, allows to describe interactions between biodegradable polymer and natural particle-shaped filler. The addition of filler influenced the overall mechanical properties of the composites, which were characterized by high stiffness and high brittleness. Significant increase of the composites' storage modulus was caused simultaneously by the presence of rigid particle-shaped structures dispersed in polymeric matrix, as well as an increase of crystallinity of polymeric matrix. It should be noticed that application of ground chestnut shell without preliminary chemical treatment allows for production by melt processing composite materials without hydrolytic degradation of the bio-polyester matrix. These composites can be used as eco-friendly, biodegradable materials for application where lower value of impact strength is acceptable. This study resulted in exploring a promising method of organic waste post-production management.

Acknowledgements The presented research results, executed under the subject of No. 02/25/DSPB/4310, were funded with Grants for education allocated by the Ministry of Science and Higher Education in Poland.

Open Access This article is distributed under the terms of the Creative Commons Attribution 4.0 International License (http://creativecommons.org/licenses/by/4.0/), which permits unrestricted use, distribution, and reproduction in any medium, provided you give appropriate credit to the original author(s) and the source, provide a link to the Creative Commons license, and indicate if changes were made.

References

1. Gołębiewski J, Gibas E, Malinowski R (2008) Selected biodegradable polymers—preparation, properties, applications. Polimery 53:799–807
2. Błędzki AK, Jaszkiewicz A (2008) Biocomposites based on polylactide reinforced with the fibers of natural origin. Polimery 53:564–570
3. Razak NIA, Ibrahim NA, Zainuddin N, Rayung M, Saad WZ (2014) The influence of chemical surface modification of kenaf fiber using hydrogen peroxide on mechanical properties of biodegradable kenfaf fiber/poly(lactic acid) composites. Molecues 19:2957–2968. doi:10.3390/molecules19032957
4. Żenkiewicz M, Richert J, Rytlewski P, Moraczewski K, Stepczyńska M, Karasiewicz T (2009) Characterisation multi-extruded poly(lactic acid). Polym Test 28:412–418. doi:10.1016/j.polymertesting.2009.01.012
5. Żenkiewicz M, Richert J (2009) Thermoforming of polylactide nanocomposite films for packing containers. Polimery 54:299–302
6. Fukushima K, Tabuani D, Arena M, Gennari M, Camino G (2013) Effect of clay type and loading on thermal, mechanical properties and biodegradation of poly(lactic acid) nanocomposites. React Funct Polym 73:540–549. doi:10.1016/j.reactfunctpolym.2013.01.003
7. Żenkiewicz M, Richert J (2008) Effect of nanofillers and sample dimensions on the mechanical properties of injection-molded polylactide nanocomposites. Polimery 53:591–594
8. Oksman K, Skrifvars M, Selin JF (2003) Natural fibers as reinforcement in polylactic acid (PLA) composites. Compos Sci Technol 63:1317–1324. doi:10.1016/S0266-3538(03)00103-9
9. Weng YX, Jin YJ, Meng QY, Wang L, Zhang M, Wang YZ (2013) Biodegradation behavior of poly(butylenes adipate-co-terephthalate) (PBAT), poly(lactic acid) (PLA), and their blend under soil conditions. Polym Test 32:918–926. doi:10.1016/j.polymertesting.2013.05.001
10. Lezak E, Kulinski Z, Masiarek R, Piórkowska E, Parcella M, Gadzinowska K (2008) Mechanical and thermal properties of green polylactide composites with natural fillers. Macromol Biosci 8:1190–1200. doi:10.1002/mabi.200800040
11. Fukushima K, Rasyida A, Yang MC (2013) Biocompatibility of organically modified nanocomposites based on PBAT. J Polym Res 20:302. doi:10.1007/s10965-013-0302-6

12. Kim JH, Lee JC, Kim GH (2015) Study on poly(butylene adipate-*co*-terephthalate)/starch composites with polymeric methylenediphenyl diisocyanate. J Appl Polym Sci 132:41884. doi:10.1002/app.41884
13. Siyamak S, Ibrahim NA, Abdolmohammadi S, Yunus WM, Rahman MZ (2012) Enhancement of mechanical and thermal properties of oil palm empty fruit bunch fiber poly(butylenes adipate-co-terephthalate) biocomposites by matrix esterification using succinic anhydride. Molecues 17:1969–1991. doi:10.3390/molecules17021969
14. Li XH, Meng YZ, Wang SJ, Varada Rajulu A, Tjong SC (2004) Study on poly(butylene adipate-*co*-terephthalate)/starch composites with polymeric methylenediphenyl diisocyanate. J Polym Sci Part B 42:666–675. doi:10.1002/polb.10761
15. Li XH, Meng YZ, Chen GQ, Li RKY (2004) Themral properties and rheological behavior of biodegradable aliphatic polycarbonate derived from carbon dioxide and propylene oxide. J Appl Polym Sci 94:711–716. doi:10.1002/app.20938
16. Xing C, Wang H, Hu Q, Xu F, Cao X, You J, Li Y (2013) Mechanical and thermal properties of eco-friendly poly(propylene carbonate)/cellulose acetate butyrate blends. Carbohydr Polym 92:1921–1927. doi:10.1016/j.carbpol.2012.11.058
17. Zdanowicz M, Spychaj T, Lendzion-Bieluń Z (2014) Crosslinked carboxymethyl starch: one step synthesis and sorption characteristics. Int J Biol Macromol 71:87–93. doi:10.1016/j.ijbiomac.2014.04.043
18. Zdanowicz M, Schmidt B, Spychaj T (2010) Starch graft copolymers as superabsorbents obtained via reactive extrusion processing. Pol J Chem Technol 12:14–17. doi:10.2478/v10026-010-0012-3
19. Zdanowicz M, Spychaj T, Mąka H (2016) Imidazole-based deep eutectic solvents for starch dissolution and plasticization. Carbohydr Polym 140:416–423. doi:10.1016/j.carbpol.2015.12.036
20. Kuciel S, Liber-Kneć A, Zajchowski S (2009) Biocomposites based on thermoplastic starch or polylactide/starch blends as the matrices filled with natural fibers. Polimery 54:667–673
21. Oksman K, Skrifvars M, Selin JF (2003) Natural fibers as reinforcement in polylactic acid (PLA) composites. Compos Sci Technol 63:1317–1324. doi:10.1016/S0266-3538(03)00103-9
22. Salasinska K, Ryszkowska J (2012) Natural fibre composites from polyethylene waste and hazelnut shell: dimensional stability, physical, mechanical and thermal properties. J Compos Interfaces 19:321–332. doi:10.1080/15685543.2012.726156
23. Sałasińska K, Ryszkowska J (2013) Dimensional stability, physical, mechanical and thermal properties of high density polyethylene with peanut hulls composites. Polimery 58:461–466. doi:10.14314/polimery.2013.461
24. Sałasińska K, Osica A, Ryszkowska J (2012) The use of tree leaves as reinforcement in composites with recycled PE-HD matrix. Polimery 57:646–655. doi:10.14314/polimery.2012.646
25. Sałasińska K, Ryszkowska J (2013) Composites of polylactic acid reinforced with plant fillers obtained from farm and food industry. Przem Chem 92:2027–2031
26. Baillie C (2004) Green composites: polymer composites and the environment. Woodhead Publishing, Cambridge
27. Kaymakci A, Ayrilmis N (2014) Waste chestnut shell as a source of reinforcing fillers for polypropylene composites. J Thermoplast Compos 27:1054–1064. doi:10.1177/0892705712461648
28. Wu CS, Hsu YC, HT Liao, Yen FS, Wang CY, Hsu CT (2014) Characterization and biocompatibility of chestnut shell fiber-based composites with polyester. J Appl Polym Sci 131:40730. doi:10.1002/app.40730
29. Menard KP (1999) Dynamic mechanical analysis: a practical introduction. CRC Press, Washington
30. Baek B-S, Park J-W, Lee B-H, Kim H-J (2013) Development and application of green composites: using coffee ground and bamboo flour. J Polym Environ 21:702–709. doi:10.1007/s10924-013-0581-3
31. Bledzki AK, Mamun AA, Volk J (2010) Barley husk and coconut shell reinforced polypropylene composites: the effect of fibre physical, chemical and surface properties. Compos Sci Technol 70:840–846. doi:10.1016/j.compscitech.2010.01.022
32. Vazquez G, Calvo M, Freire MS, Gonzalez-Alvarez J (2009) Chestnut shell as heavy metal adsorbent: optimization study of lead, copper and zinc cations removal. J Hazard Mater 172:1402–1414. doi:10.1016/j.jhazmat.2009.08.006
33. Tsou C-H, Suen M-C, Yao W-H, Yeh J-T, Wu C-S, Tsou C-Y, Chiu S-H, Chen J-C, Wang RY, Lin S-M, Hung W-S, De Guzman M, Hu C-C, Lee K-R (2014) Preparation and characterization of bioplastic-based green renewable composites from tapioca with acetyl tributyl citrate as a plasticizer. Materials 7(8):5617–5632. doi:10.3390/ma7085617
34. Qu P, Gao Y, G-f Wu, L-p Zhang (2010) Nanocomposites of poly(lactic acid) reinforced with cellulose nanofibrils. Bioresources 5:1811–1823
35. Zhang J, Sato H, Tsuji H, Noda I, Ozaki Y (2005) Differences in the CH3···O=C interactions among poly(L-lactide), poly(L-lactide)/poly(D-lactide) stereocomplex, and poly(3-hydroxybutyrate) studied by infrared spectroscopy. J Mol Struct 735–736:249–257. doi:10.1016/j.molstruc.2004.11.033
36. Carrascoa F, Pages P, Gámez-Pérez J, Santana OO, Maspoch ML (2010) Processing of poly(lactic acid): characterization of chemical structure, thermal stability and mechanical properties. Polym Degrad Stab 95:116–125. doi:10.1016/j.polymdegradstab.2009.11.045
37. Ndazi BS, Karlsson S (2011) Characterization of hydrolytic degradation of polylactic acid/rice hulls composites in water at different temperatures. Express Polym Lett 5:119–131. doi:10.3144/expresspolymlett.2011.13
38. Sawai D, Takayashi K, Imamura T, Nakamura K, Kanamoto T, Hyon SH (2002) Preparation of oriented β-form poly(L-lactic acid) by solid-state extrusion. J Polym Sci Part B 40:95–104. doi:10.1002/polb.10076
39. Ouchiar S, Stoclet G, Cabaret C, Gloaguen V (2016) Influence of the filler nature on the crystalline structure of polylactide-based nanocomposites: new insights into the nucleating effect. Macromolecules 49:2782–2790. doi:10.1021/acs.macromol.5b02746
40. Nyambo C, Mohanty AK, Misra M (2010) Polylactide-based renewable green composites from agricultural residues and their hybrids. Biomacromolecules 11:1654–1660. doi:10.1021/bm1003114
41. Fu S-Y, Feng X-Q, Lauke B, Mai Y-W (2008) Effects of particle size, particle/matrix interface adhesion and particle loading on mechanical properties of particulate–polymer composites. Compos Part B Eng 39:933–961. doi:10.1016/j.compositesb.2008.01.002
42. Brostow W, Hagg Lobland HE, Narkis MJ (2006) Sliding wear, viscoelasticity, and brittleness of polymers. Mater Res 21:2422–2428. doi:10.1557/JMR.2006.0300
43. Wallenberger TF, Weston N (2011) Natural fibers, plastics and composites. Springer, New York
44. Barnes HA, Hutton JF, Walters FRS (1993) An introduction to rheology. Elsevier, Tokyo
45. Pothana LA, Oommennb Z, Thomas S (2003) Dynamic mechanical analysis of banana fiber reinforced polyester composites. Compos Sci Technol 63:283–293. doi:10.1016/S0266-3538(02)00254-3
46. Eng CC, Ibrahim NA, Zainuddin N, Ariffin H, Yunus WMZW, Then YY (2014) Enhancement of mechanical and dynamic mechanical properties of hydrophilic nanoclay reinforced polylactic acid/polycaprolactone/oil palm mesocarp fiber hybrid composites. Int J Polym Sci. doi:10.1155/2014/715801
47. Liu W, Misra M, Askeland P, Drzal LT, Mohanty AK (2005) 'Green' composites from soy based plastic and pineapple leaf fiber: fabrication and properties evaluation. Polymer 46:2710–2721. doi:10.1016/j.polymer.2005.01.027